OPTOELECTRONICS AND ADVANCED MATERIALS – RAPID COMMUNICATIONS Vol. 17, No. 11-12, November-December 2023, p. 484-489

Analysis of temperature sensitivity of fibers with high nonlinear characteristics in Rayleigh backscattering based OTDR temperature sensor

ABDULLAH ERKAM GUNDUZ[1,*], HALİM HALDUN GOKTAS[2]
[1]*Department of Electrical and Electronics Engineering, Ankara Yıldırım Beyazıt University, Ankara, Turkiye*
[2]*Department of Electrical and Electronics Engineering, Ankara Bilim University, Ankara, Turkiye*

This paper presents an investigation of different types of fibers for their compatibility in a Rayleigh based optical time domain reflectometer (R-OTDR) temperature sensor setup. A reference test setup consisting of standard single mode fiber (SMF) is observed to constitute a background for comparison. In this setup, the Rayleigh response of -50.25 dBm and a temperature sensitivity of 0.002 dB/°C is achieved. Then Rayleigh responses for highly nonlinear fiber (HNLF), dispersion shifted fiber (DSF) and polarization maintaining fiber (PMF) are observed. The Rayleigh responses were: HNLF had -39.83 dBm, DSF had -34.03 dBm and PMF had -31.34 dBm. Since PMF showed the best Rayleigh response it was selected to be observed as fiber under test (FUT) in a classical R-OTDR temperature sensor setup. With the PMF used in temperature R-OTDR setup a temperature sensitivity of 0.018 dB/°C was achieved. As a result, it has been determined that PMF fiber has high temperature sensitivity in R-OTDR installations compared to SMF. It has been shown that temperature measurements can be made on shorter lengths of fiber with a much simpler setup using PMF as opposed to the more complex alternatives.

(Received June 9, 2023; accepted December 4, 2023)

Keywords: Optical time domain reflectometer, Rayleigh backscattering, Distributed temperature sensor, Nonlinear fiber

1. Introduction

The simplicity, accuracy and higher sustainability of optical fiber sensors have attracted many researchers to apply them in temperature sensing applications [1,2]. Various methods of optical fiber sensors have been investigated in the literature, mainly; Fiber Bragg Grating (FBG) based [3-6], Brillouin backscattering based [7-11] and Raman backscattering based [12-14]. However, Rayleigh backscattering based [15-17] fiber optic temperature sensors offer more advantages as they are much simpler and cheaper.

Brillouin backscattering based temperature sensors offer advantages in sensitivity [18,19]. However, the frequency analysis in Brillouin sensors require many filters, window fittings, complex calculations of reverse Fourier transform even before the data becomes usable for processing [20,21]. FBG based sensors also suffer from the same frequency analysis complexity [22]. Although they are mainly used in fiber amplifiers [23-25], Raman backscattering can also be utilized in temperature sensing. However, Raman sensors need powerful amplifiers and polarization controllers [26], which add to the overall cost the sensor setup. In Rayleigh based setups, on the other hand, especially in classical OTDR's, depending on the selection of the test fiber type good temperature results can be achieved even with shorter lengths of FUT [27]. Thereby, Rayleigh based sensors offer more accessible and easier alternatives to inelastic backscattering sensors.

There are various types of Rayleigh based fiber optic temperature sensors. Yang Zhi et al., proposed a system that utilized the jagged appearance of Rayleigh backscatter traces from an SMF measured with a coherent OTDR (COTDR) that was dependent on the reproducibility and restorability of the Rayleigh backscatter traces. When the system was simulated the frequency compensation for strain and temperature change is detected through cross correlation of reference OTDR signal and measured OTDR signal [28].

Leonardo Marcon et al., proposed an OTDR system modelled with the virtual perturbation induced by the cumulative round-trip time delay change. The model works by comparing the theoretical results obtained from the first section of the fiber which is subjected to temperature change to the virtual perturbations measured on the second section of the fiber. For each measured disturbance an algorithm can compute and correct the corresponding virtual perturbation, improving the quality of the CP phase-OTDR [29].

Tao Liu et al., demonstrated an ultra-high resolution distributed strain sensor assisted with Rayleigh-scattering enhanced optical fiber and phase noise compensation scheme. They achieved a static strain resolution of 1.89 nε and dynamic resolution of 97.5 pε/√Hz over 1Hz [30].

Chengli Li et al., proposed an enhanced distributed optical fiber sensor based on broadband ultra-weak fiber Bragg grating array (UWFBG) to measure dynamic strain using −50 dB reflectivity and with reflected signal 17 dB

higher than the Rayleigh backscattering. They successfully managed to observe a temperature range of 20 °C to 200 °C with minimum phase detection of 1.02×10^{-3} rad/Hz, and SNR above 59.2 dB at 100 Hz [31].

Although COTDR based sensors offer good results, the complexity of the sensor setup and high processing power needed for data analysis remain major problems. This is why a simpler classical R-OTDR system can be chosen as alternative temperature sensor.

The temperature sensitivity response of an R-OTDR sensor is highly dependent of the type of fiber used as FUT. Fibers with higher Rayleigh backscattering characteristics can be utilized to improve the temperature sensitivity. Therefore, observing different types of fibers for their Rayleigh responses would provide us with answers to if any accessible and cheap fibers can be used as testing medium.

In this paper, different types of nonlinear fibers, namely, HNLF, DSF and PMF are tested for their suitability as a potential R-OTDR temperature sensor medium. First, the Rayleigh backscattering characteristics of these fibers are observed and compared with a SMF. Then, 50 m of the fiber with the best Rayleigh backscattering characteristic is tested in a classical R-OTDR temperature sensor setup. The resulting temperature sensitivity is compared with that of SMF.

2. Theoretical analysis of R-OTDR

The Rayleigh backscattering constitutes an important part of the fiber losses during light transmission. The medium of a fiber is not perfectly homogeneous, however, with thermal and strenuous effects during the fabrication process inhomogeneities form. These molecular inhomogeneities along the fiber cause transmitted light to be reflected. These reflections are elastic ones as opposed to Brillouin and Raman reflections, meaning they are of the same frequency as the incident light. The Rayleigh scattering coefficient is given by equation (1) [32]:

$$\alpha = \frac{8b\pi^3}{3\lambda^4}(n^2-1)kT\beta \quad (1)$$

where β is the isothermal compressibility, λ is the wavelength, k is the Boltzmann constant, T is the ambient temperature and n is the refractive index.

By putting an incident pulsed light at the source, the backscattered reflections can be located and monitored as different amplitudes will be observed coming from different locations on the fiber. If the light at the source has peak power P_0 and pulse width τ then the power of the reflected back Rayleigh signal from any location on the fiber can be found with equation (2):

$$P_s(t) = (1-\kappa)\kappa P_0 Dr(z) exp\{-\int_0^z 2\alpha_i(z)dz\} \quad (2)$$

where the time can be converted to location by z = ct/2n, as the light would propagate twice the distance going back and forth. $\alpha_i(z)$ is the attenuation coefficient in nepers. D = (ct/n) is the length of the optical pulse in the fiber at any instant in time. If we take the slope of the logarithmic power of the reflected back signal, it's clear that it's directly related to attenuation coefficient by equation (3):

$$\frac{\partial(\ln P_s)}{\partial z} = -2\alpha_i(z) \quad (3)$$

3. Rayleigh spectra for different fibers

The tuneable laser source is connected to the 3-port circulator and then to the fiber under test. The circulator can operate in S+C+L band wavelength regions. The reflected back Rayleigh signal passes from the second port of the circulator to the third port. From there the signal reaches optical spectrum analyser to be observed. The laser source is set to span wavelengths from 1530 nm to 1580 nm at -5 dBm power. The FUT is changed as: SMF (1 km), DSF (1 km), PMF (1 km) and HNLF (1 km). The setup is given in Fig. 1.

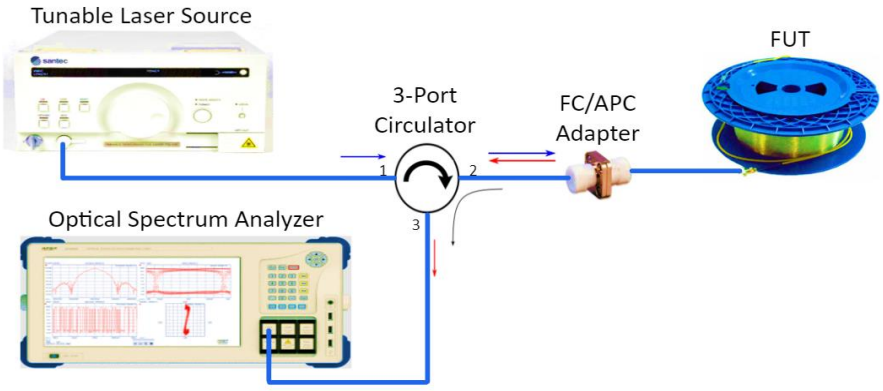

Fig. 1. Rayleigh spectra test setup (color online)

The results are shown in Fig. 2. Although the HNLF yields promising Rayleigh backscattering signal at -39.83 dBm power, PMF offers the best response at -31.34 dBm.

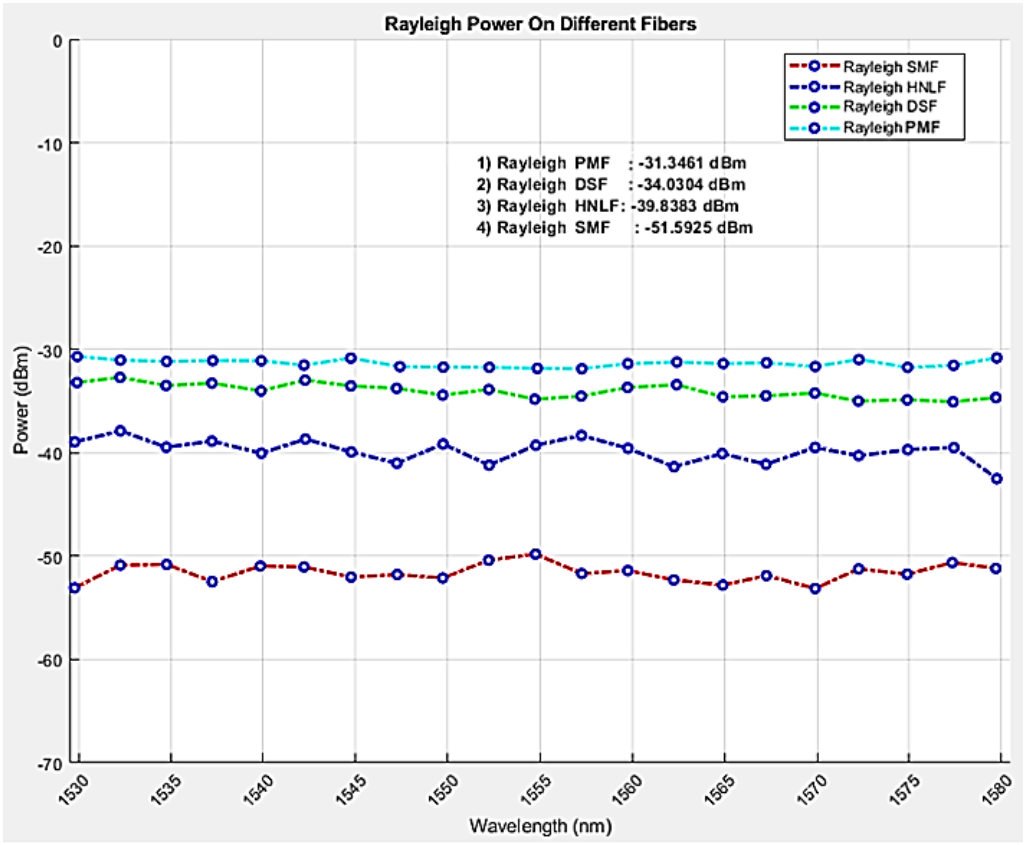

Fig. 2. Rayleigh response results for SMF (1km), DSF (1km), PMF (1km) and HNLF (1km) (color online)

Since the PMF has the best Rayleigh response, it is tested in R-OTDR temperature sensor as 50 m FUT and its temperature response is compared to that of 50 m SMF FUT.

4. R-OTDR temperature test results

The FUT are cut into 50 m segments for both SMF and PMF. They are put on the temperature test setup given in Fig. 3. The optical pulse generator (RF Optics) generates 1550 nm optical pulse signals which can be triggered either internally or externally. When the internal trigger is activated, the laser works with on-board modulator to produce optical pulse in the limit of 50 ns pulse width and 5 kHz repetition rate. The external trigger enables the laser to be modulated via a Low Frequency (LF) electrical pulse. An LF signal generator (Agilent 33500B) is used to trigger the pulse laser. The channel 1 output of the signal generator is connected to pulse laser external trigger input. The laser output is connected to EDFA1 (YİMİ, tuneable EDFA) which can generate up to 30 dB gain and is capable of stabilizing temperature for long periods of time. The EDFA1 current was set to 275 mA, which corresponded to 22 dB gain. The amplified optical pulse is then sent to the FUT via a S+C+L wideband 3-port circulator. The pulse goes through circulator's port 1 to port 2 then onto the FUT. Here the FUT is divided into two segments; first a 2.275 km initial SMF which is used to mitigate the event dead zone of OTDR and to simulate a temperature event observed from a distance, then a 50 m temperature FUT segment. The reflected Rayleigh signal is then sent to Photo Diode (P.D) via circulator's port 2 to port 3. Same as the optical pulse, the reflected Rayleigh signal was around -20 dB in power, which was not detectable by the P.D. EDFA 2 (YİMİ brand, fixed power EDFA) is used to amplify the signal with a fixed gain of around 20 dB. Finally, the amplified Rayleigh signal arrives at the P.D to be converted into electrical signal. Then the converted electrical signal is sent to a high sampling rate oscilloscope (Agilent MSO-X 3054-A, up to 4 GSa/s).

After the oscilloscope the signal arrives at the computer port and data is processed by MATLAB program. The program first clears all existing connections, if any. Then it connects to the oscilloscope via visa object and sets both input and output buffers. Then it connects to signal generator and optical pulse generator in that order. The signal generator is then sent the desired pulse width and repetition rate. Then pulse generator internal trigger is deactivated and is triggered with signal generator pulse. The pulse laser output is turned on. After a warmup period of 10 seconds, the oscilloscope is activated to acquire a window reading. The acquired data is then turned into numeric form and displayed on the screen. Since all the filtering, fitting, and averaging is done over the oscilloscope, no further data processing is needed. The flowchart of the program is given in Fig. 4.

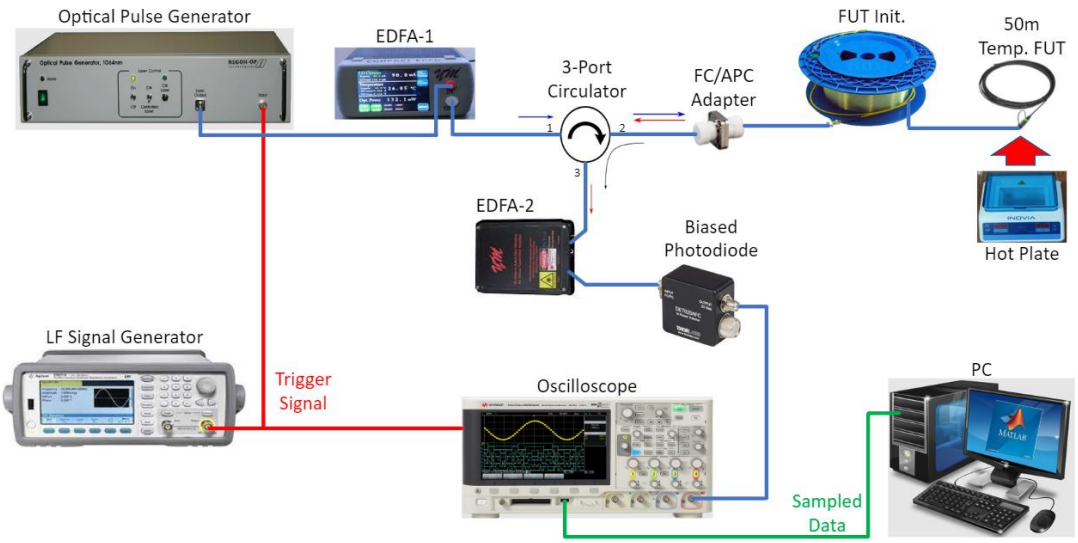

Fig. 3. R-OTDR Temperature Sensor test setup. (LF: Low Frequency) (color online)

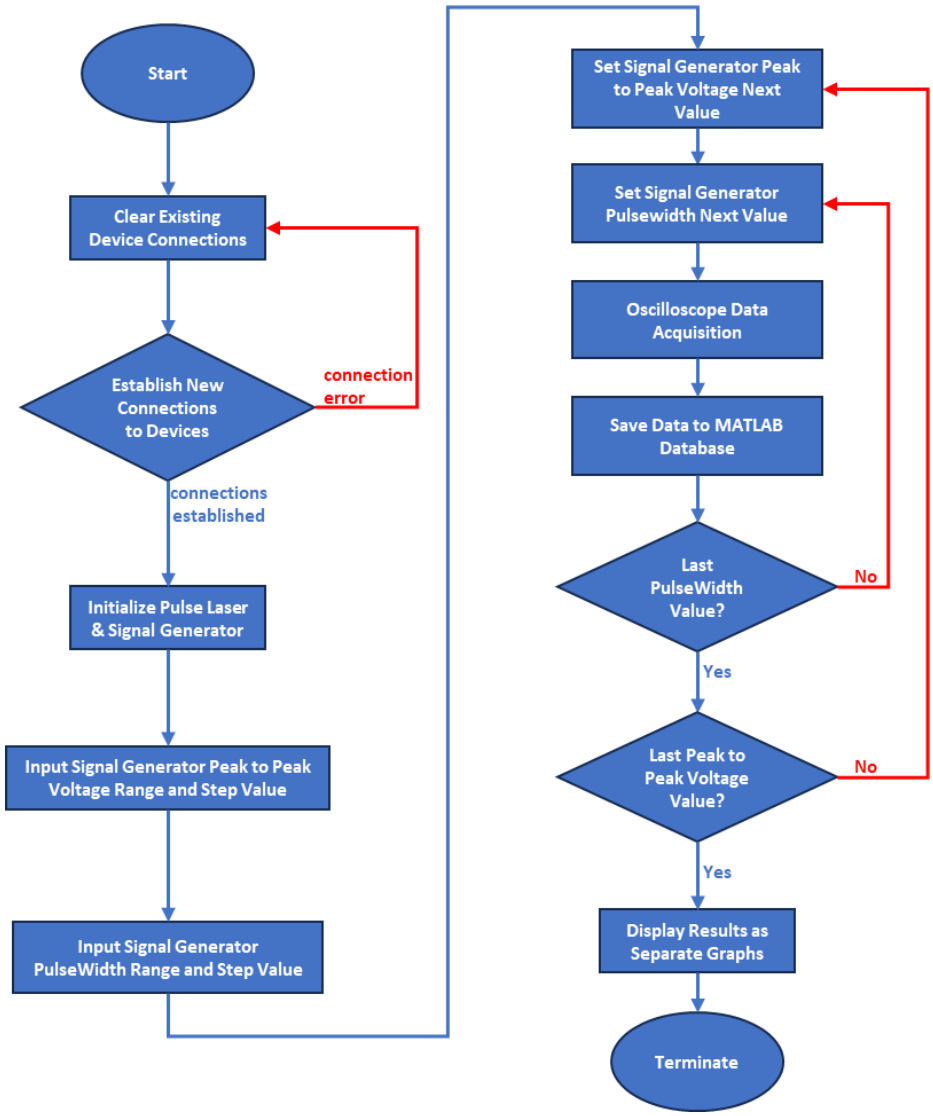

Fig. 4. Flowchart of the MATLAB program

Using the fully automated program the experiments have been repeated 100 times for each temperature value and the results are averaged.

The spatial resolution of the proposed setup is calculated with equation (4):

$$SR = \frac{c\tau}{2n} \quad (4)$$

where pulse width τ is 50 nm. Which gives us a spatial resolution of approximately 5 m.

The results for the 50 m SMF segment placed inside hotplate are given in Fig. 5. The hot plate temperature is changed respectively as 20 °C, 40 °C, 60 °C, 80 °C and 100 °C. The hotplate stayed at each temperature interval for over 10 minutes to get accurate repeatability of the experiment. The Rayleigh peak results are 20 °C -6.72 dB, 40 °C -6.68 dB, 60 °C -6.64 dB, 80 °C -6.61dB and 100 °C -6.56 dB.

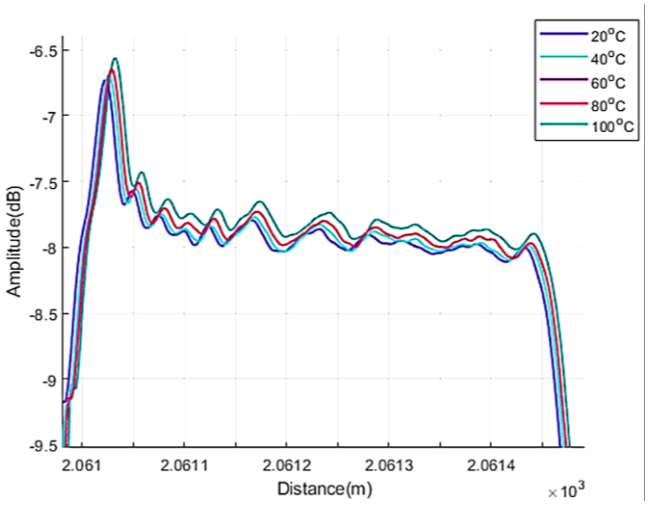

(a) Rayleigh response of 50 m SMF vs temperature

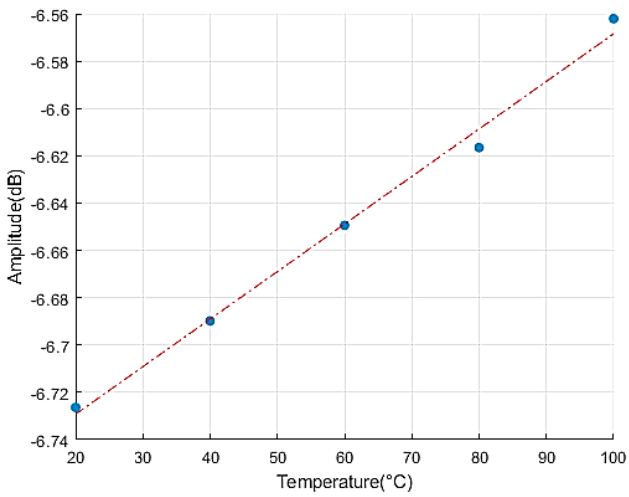

(b) Rayleigh peak points vs. temperature

Fig. 5. Rayleigh response of SMF vs temperature (color online)

The linearity (R^2) of Fig. 5(b) is found as 0.9954.

Finally, the experiment is repeated for 50 m PMF segment with splice in between. The results are given in Fig. 6. The Rayleigh peak results are 20 °C -29.3118 dB, 40 °C -28.8579 dB, 60 °C -28.6929 dB, 80 °C -28.2343 dB and 100 °C -27.9739 dB.

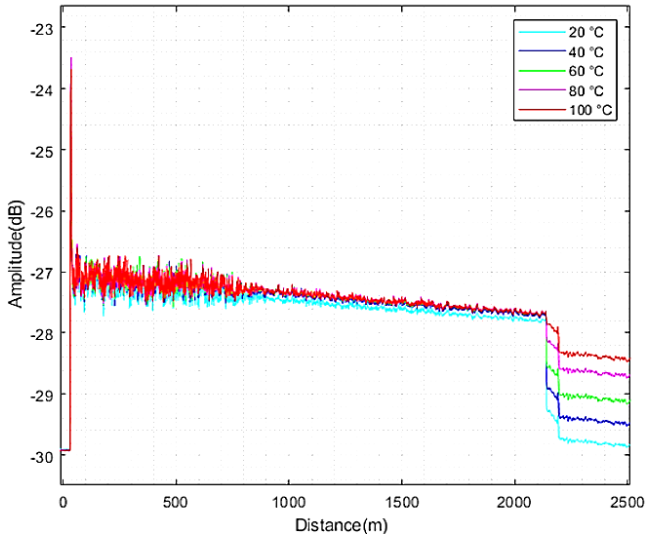

(a) Rayleigh response of 50 m PMF vs. temperature

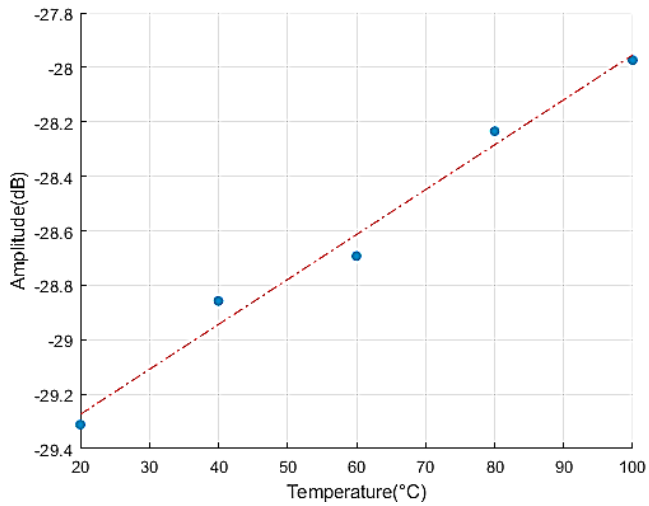

(b) Rayleigh peak points vs. temperature

Fig. 6. Rayleigh response of PMF vs temperature (color online)

The linearity (R^2) of Fig. 6(b) is found as 0.9838.

The splice point drops can be clearly seen in Fig. 6. As stated above, these drop points have different values depending on the temperature. The temperature response is improved to 0.018 dB/°C.

5. Conclusion

In this study it has been investigated to make a simpler fiber optic temperature sensor compared to FBG, Brillouin and Raman based sensors. A classical R-OTDR temperature sensor is investigated as it is much easier to setup compared to COTDR setups.

As the type of the FUT would directly affect the temperature sensitivity, different types of candidate fibers are observed in an R-OTDR setup. First, Rayleigh backscattering responses for SMF (1 km), DSF (1 km), PMF (1 km) and HNLF (1 km) segments were observed. The Rayleigh responses were: HNLF had -39.83 dBm, DSF had -34.03 dBm and PMF had -31.34 dBm. The PMF fiber segment showed the most promise among other fibers to be applied as a temperature sensing medium.

Then temperature sensitivity for 50 m SMF and PMF sections are observed in R-OTDR setup. The fiber attenuations and splice point drops for different temperatures were observed. The SMF segment had temperature sensitivity of 0.002 dB/°C, whereas the PMF had temperature sensitivity of 0.018 dB/°C.

Just by changing the FUT type to PMF a 10 times improvement was achieved in the temperature sensitivity. A small FUT length of just 50 m was used. Compared to other types of fiber sensors, no excessive data or frequency domain analysis was needed. Only averaging and a simple fitting was applied. This significantly reduced the computational power needed.

Overall, this study showed that the complexities of the bulky, long fiber temperature sensors can be reduced with a simple R-OTDR based sensor which uses an alternative fiber PMF with a good Rayleigh backscattering response.

References

[1] E. Udd, Rev. Sci. Instrum. **66**, 4015 (1995).
[2] K. T. V. Grattan, T. Sun, Sensor Actuat. A-Phys. **82**(1-3), 40 (2000).
[3] M. Yücel, N. F. Öztürk, M. Yücel, H. H. Göktaş, A. E. Gündüz, Optik, Sig. Process Commun. **24**, 669 (2016).
[4] M. Yücel, N. F. Öztürk, M. Torun, M. Yücel, Journal of the Faculty of Engineering and Architecture of Gazi University **32**(3), 957 (2017).
[5] S. E. Kipriksiz, M. Yücel, Opt. Quant. Electron. **53**(6), 1 (2021).
[6] M. Yücel, N. F. Öztürk, Instrum. Sci. Technol. **46**(5), 519 (2018).
[7] M. Yücel, H. H. Göktaş, M. Yücel, N. F. Öztürk, A. E. Gündüz, Turk. J. Electr. Eng. Co. **25**(5), 3881 (2017).
[8] M. Yücel, M. Yücel, N. F. Öztürk, H. H. Göktaş, Sig. Process Commun. **23**, 632 (2015).
[9] N. M. Yücel, M. Yücel, A. E. Gündüz, H. H. Göktaş, N. F. Öztürk, Sig. Process Commun. **24**, 461 (2016).
[10] M. Yücel, H. H. Göktaş, N. F. Öztürk, Sig. Process Commun. **22**, 838 (2014).
[11] M. Yücel, M. Yücel, Microw. Opt. Techn. Let. **64**(1), 190 (2022).
[12] M. Yonas, O. J. Claudio, D. P. Fabrizio, AIP Conf. Proc. **7**, 1 (2019).
[13] M. K. Saxena, S. D. V. S. J. Raju, R. Arya, R. B. Pachori, S. V. G. Ravindranath, S. Kher, S. M. Oak, Opt. Laser Technol. **65**, 14 (2015).
[14] Z. Wang, X. H. Sun, Q. Xue, Y. L. Wang, Y. L. Qi, X. S. Wang, Opt. Laser Technol. **93**, 224 (2017).
[15] X. Bao, Y. Wang, Advanced Devices & Instrumentation **2021**, 1 (2021).
[16] L. Palmieri, L. Schenato, M. Santagiustina, A. Galtarossa, Sensors **22**, 6811 (2022).
[17] D. K. Gifford, B. J. Soller, M. S. Wolfe, M. E. Froggatt, 31st European Conference on Optical Communication, **31**(3), 511 (2005).
[18] V. L. Iezzi, S. Loranger, M. Marois, R. Kashyap, Opt. Lett. **39**, 857 (2014).
[19] L. Qiu, Z. Zhu, T. Li, D. Zhou, Y. Dong, IEEE Sens. J. **21**(5), 6209 (2021).
[20] A. Minardo, R. Bernini, R. R. Lombera, J. Mirapeix, J. M. L. Higuera, L. Zeni, Opt. Express **24**, 29994 (2016).
[21] C. Karapanagiotis, A. Wosniok, K. Hicke, K. Krebber, Sensors **21**, 2724 (2021).
[22] M. Zaynetdinov, E. M. See, B. Geist, G. Ciovati, H. D. Robinson, V. Kochergin, IEEE Sens. J. **15**(3), 1908 (2015).
[23] I. A. Gurkaynak, T. F. Al-Mashhadani, M. K. S. Al-Mashhadani, M. H. Ali, A. E. Gunduz, M. Yucel, H. H. Göktaş, K. A. Zidan, Microw. Opt. Techn. Let. **64**(2), 251 (2022).
[24] I. A. Gurkaynak, M. K. S. Al-Mashhadani, M. H. Ali, T. F. Al-Mashhadani, A. E. Gunduz, M. Yucel, H. H. Göktaş, Opt. Quant. Elecetron. **53**(7), 1 (2021).
[25] I. A. Gurkaynak, T. F. Al-Mashhadani, M. Yucel, H. H. Goktas, 8th International Conference on Electrical and Electronics Engineering (ICEEE) **8**, 32 (2021).
[26] Z. Zhang, H. Wu, C. Zhao, M. Tang, J. Lightwave Technol. **39**(2), 654 (2021).
[27] M. Ohashi, H. Kubota, Y. Miyoshi, 2020 Opto-Electronics and Communications Conference (OECC) **25**, 1 (2020).
[28] Y. Zhi, S. Pengxiang, L. Yongqian, 2011 Second International Conference on Mechanic Automation and Control Engineering **2**, 590 (2011).
[29] L. Marcon, M. Soriano-Amat, R. Veronese, A. Garcia-Ruiz, M. Calabrese, L. Costa, M. R. Fernandez-Ruiz, H. F. Martins, L. Palmieri, M. Gonzalez-Herraez, IEEE Photonic Tech. L. **32**(3), 158 (2020).
[30] T. Liu, H. Li, F. Ai, J. Wang, C. Fan, Y. Luo, Z. Yan, D. Liu, Q. Sun, 2019 Optical Fiber Communications Conference and Exhibition (OFC) **1**, 1 (2019).
[31] C. Li, J. Tang, Y. Jiang, C. Cheng, L. Cai, M. Yang, IEEE Photonics J. **12**(4), 1 (2020).
[32] D. B. Keck, "Optical Fiber Waveguides", Academic Press, New York, 1980.

*Corresponding author: aegunduz@aybu.edu.tr